Supplementary Information for

Trade-off between O_2 activation and active-site regeneration on biaxially strained Co-doped MoS_2 monolayers: a density functional theory study

Soon-Dong Park [a] and Sung Youb Kim [a,b] *

[a] Graduate School of Carbon Neutrality, Ulsan National Institute of Science and Technology, Ulsan 44919, Republic of Korea
[b] Graduate School of Semiconductor Materials and Devices Engineering, Ulsan National Institute of Science and Technology, Ulsan 44919, Republic of Korea

* Corresponding author: sykim@unist.ac.kr

Table S1. O–O stretching frequencies (ν_{O-O}) for O_2 adsorbed at the Co substitutional site (Co@V_S) in monolayer MoS_2 under biaxial tensile strain (ε = 0–10%). The data include both S-preserved (SP) and S-reconstructed (SR) adsorption configurations, as well as their coexistence at ε = 4.5%. The experimental equilibrium stretching frequency of gas-phase O_2 is 1556 cm^{-1},[53] while our PBE calculation predicts 1567 cm^{-1} at an equilibrium bond length of 1.233 Å, indicating good agreement.

Strain	Configuration	ν_{O-O} (cm^{-1})
0.000	SP	1057.334
0.020	SP	1046.939
0.040	SP	1034.964
0.045	SP	1032.449
0.045	SR	988.309
0.075	SR	992.290
0.100	SR	998.243

For the adsorbed configurations, the O–O stretching frequencies reported in Table S1 correspond to a local O–O stretching mode, obtained by displacing only the two O atoms along the O–O bond direction while keeping the MoS_2 substrate and the Co atom fixed.

Table S2. Strain dependence of the Co–O bond strength during Steps IV–V (lateral diffusion of the Co-bound O to a neighboring S site), quantified by −ICOHP (integrated up to the Fermi level) as obtained from LOBSTER for the initial state of Step IV. A larger −ICOHP value indicates a stronger Co–O interaction.

Strain	−ICOHP
0.000	4.885
0.055	5.821

Table S3. PBE+U sensitivity test results for the Co@V_S–O_2 system (U_{eff} = 3.3 eV for Co *d* electrons, following Oh et al.[49]). $E_{SR} - E_{SP}$ is the energy difference between the SR and SP configurations at each strain. A negative value indicates that the SR configuration is thermodynamically favored.

Strain	SR converged?	M_{tot} (SR) (μ_B)	$E_{SR} - E_{SP}$ (eV)
0.000	No (collapses to SP)		
0.045	YES	~1	+0.56
0.050	Yes	~1	+0.43
0.055	Yes	~1	+0.29

Under PBE+U, the SP–SR crossover is estimated to shift to approximately 7% by linear extrapolation of the $E_{SR} - E_{SP}$ trend, compared to approximately 4.5% under PBE. However, the SR configuration remains a well-defined metastable minimum at all tested strains with the expected low-spin magnetic moment (~1 μ_B), and the energy difference decreases monotonically with strain, confirming that the same strain-driven crossover mechanism is preserved. At zero strain, the PBE and PBE+U results yield consistent structural and magnetic properties. No consensus U value has been calibrated specifically for TM@V_S configurations in MoS_2, and the quantitative crossover strain is therefore sensitive to this parameter, while the qualitative activation–regeneration trade-off mechanism remains valid.

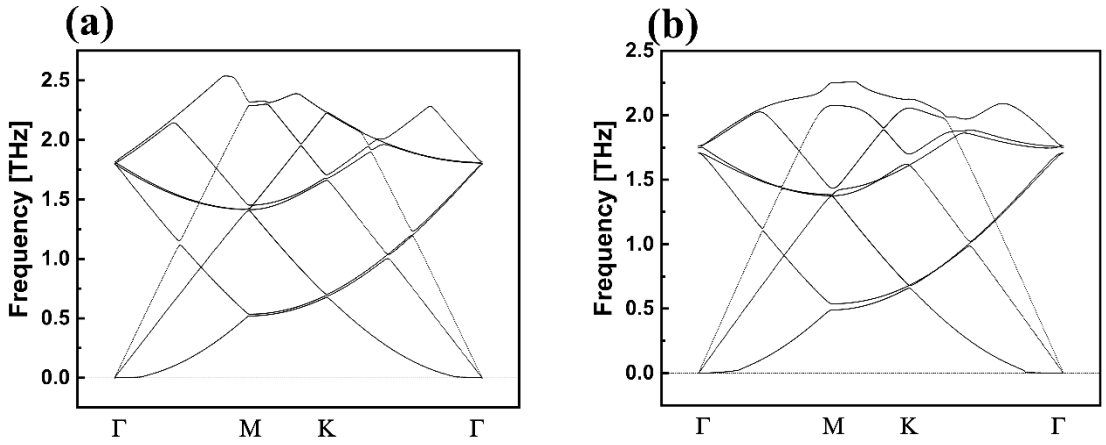

Figure S1. Phonon dispersion curves of monolayer MoS_2 under 10% biaxial tensile strain for (a) a single sulfur vacancy (V_S) and (b) a substitutional Co atom at the sulfur vacancy site (Co@V_S).

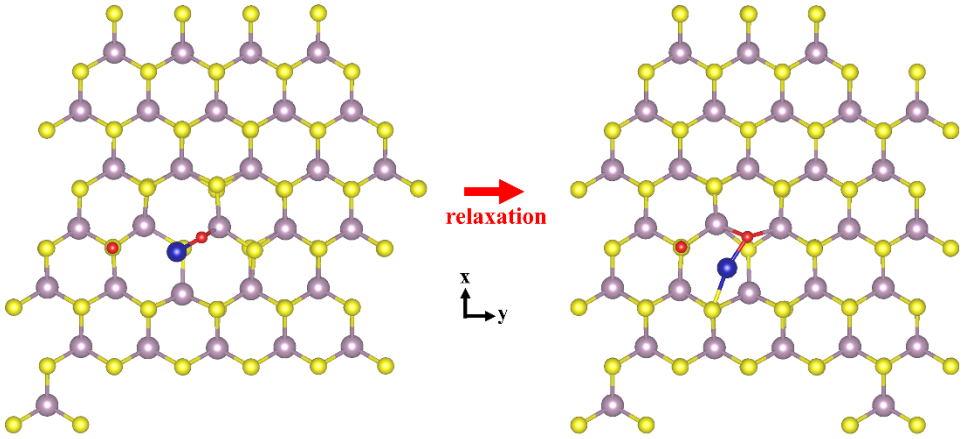

Figure S2. Active-site disruption caused by subsurface oxygen penetration at lower biaxial tensile strains. Representative snapshots during structural relaxation reveal that, starting from the post-dissociation configuration, the remaining O atom migrates into the subsurface region and displaces the Co dopant, triggering an irreversible local reconstruction (shown here for ε = 4.5%). Similar trap-forming behavior is also observed at ε = 5.0% for the same initial configuration. In contrast, at $\varepsilon \geq 5.5\%$, the O atom remains stabilized at the Co-top site without causing such disruption, resulting in a well-defined, intact intermediate that serves as the starting point for the regeneration pathway.

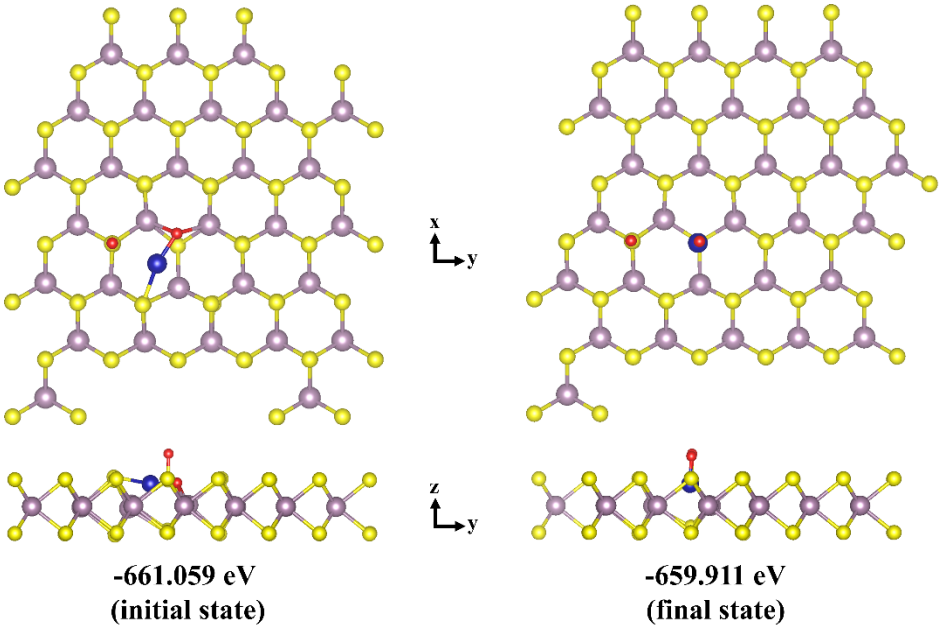

Figure S3. Energetic penalty for escaping the penetrated Co–O–Mo trap at ε = 4.5%. The structure shown is a representative snapshot at this strain. Similar energy comparisons were also conducted at ε = 5.0%, and the resulting ΔE values are summarized below.

On the left, the relaxed dissociation product transforms into a penetrated Co–O–Mo motif, representing a trapped (disrupted) configuration accompanied by significant local rearrangement. On the right, representative recovery endpoints are presented as candidate states for initiating subsequent lateral migration, in which one O atom is relocated to the Co-top position. The numbers below each snapshot indicate the total energies (in eV) of the corresponding optimized structures (rounded to three decimal places), calculated using the same 5×3 MoS_2 supercell and DFT settings. Relative energies are defined as $\Delta E = E_{end} - E_{trap}$, resulting in values of approximately 1.15 and 1.23 at strain levels ε = 4.5% and 5.0%, respectively. These positive ΔE values suggest that escaping the penetrated Co–O–Mo trap is thermodynamically unfavorable within the ε = 4.5–5.0% range in our lattice-oxygen-migration proxy for regeneration, and they indicate a substantial energetic penalty for recovery.

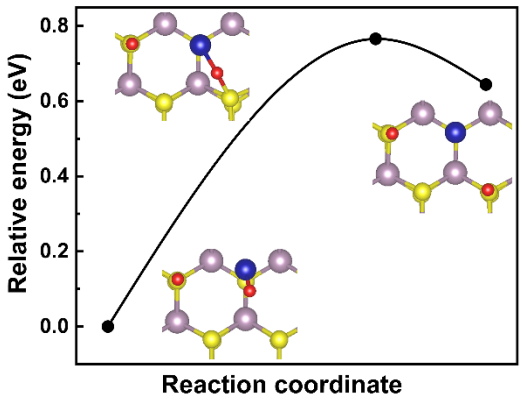

Figure S4. Minimum-energy pathway for the lateral diffusion of a Co-bound oxygen atom to a neighboring S site on Co-doped MoS_2 under zero strain (ε = 0%). The calculated activation barrier is approximately 0.77 eV. In comparison, the barrier increases to 1.63 eV at a tensile strain of ε = 5.5% (Figure 6), demonstrating that tensile strain significantly raises the energy required for oxygen removal and thus impedes active-site regeneration.